Hydrogen in oxide semiconductors

Matthew D. McCluskey,[a] Marianne C. Tarun, and Samuel T. Teklemichael
Department of Physics and Astronomy, Washington State University, Pullman, Washington 99164-2814

(Received 14 February 2012; accepted 29 March 2012)

Oxide semiconductors exhibit a range of physical properties and have potential optical, electronic, and energy applications. Transparent conducting oxides (TCOs) are currently used in products such as flat-panel displays. The prevailing *n*-type conductivity in these materials has historically been attributed to native defects such as oxygen vacancies. Recent calculations and experiments, however, have provided evidence that native defects are actually not responsible in majority of the cases. Hydrogen, on the other hand, does act as a shallow donor and can dramatically affect the electrical properties of oxides. In addition to contributing to *n*-type doping, hydrogen also passivates dangling bonds in cation vacancies and passivates acceptor dopants. Some oxides contain "hidden hydrogen," perhaps H_2 molecules, which dissociate at elevated temperatures. In this article, the many roles of hydrogen in zinc oxide, tin dioxide, titanium dioxide, indium (III) oxide, gallium (III) oxide, and strontium titanate are reviewed. The emphasis is on fundamental electronic, structural, and vibrational properties of hydrogen complexes, as determined by experiment and theory.

I. INTRODUCTION

Oxide semiconductors and insulators are currently found in a broad range of products and are on the horizon for future optical, electronic, and energy applications. The diverse range of physical properties exhibited by oxides offer nearly limitless possibilities for electronic devices.[1] Oxides show novel phenomena such as high-temperature superconductivity,[2] ferroelectricity,[3] and colossal magnetoresistance.[4] These materials exhibit complex phase behavior that depends on temperature, doping, or the application of stress. Furthermore, interfaces between different oxides produce unexpected properties. The interface between insulating strontium titanate ($SrTiO_3$) and lanthanum aluminate ($LaAlO_3$), for example, forms a highly conductive layer.[5]

One class of material, transparent conducting oxides (TCOs), combines two features that are not typically found in the same substance, electrical conductivity and optical transparency.[6] Whereas *p*-type TCOs do exist,[7] *n*-type conductivity is more common. Tin oxide (SnO_2), doped *n*-type with antimony on the substitutional tin site or fluorine on the oxygen site, is used as a coating on low-emissivity windows and heated freezer windows.[8] A dominant market for TCOs is provided by flat-panel displays. These ubiquitous devices use indium (III) oxide (In_2O_3) doped with tin (Sn) donors, referred to as indium tin oxide (ITO), as a transparent electrode. ITO is also used as the front contact in photovoltaic solar cells.[9] The market for ITO is so large that demand for indium has caused the price of that scarce commodity to increase significantly. The high cost of indium has stimulated interest in alternative materials such as SnO_2, gallium (III) oxide (Ga_2O_3), and zinc oxide (ZnO).[10]

The origin of *n*-type conductivity in TCOs is a subject of controversy.[11] Thin films of In_2O_3 without intentional doping often show free-carrier concentrations in the 10^{20} cm^{-3} range.[12] The prevalence of such high carrier concentrations has historically been explained by native defects; namely, oxygen vacancies and cation (indium) interstitials. However, the culpability of these "usual suspects" has been challenged by density functional theory (DFT) calculations. For a range of TCOs, these calculations indicate that the oxygen vacancy is a deep donor, whereas interstitials are too mobile to be stable at room temperature.[13] As discussed further in this article, hydrogen is a common contaminant that can lead to *n*-type doping.

A second possible source of *n*-type conductivity is surface defects. Photoemission spectroscopy experiments have shown that the surface Fermi level lies within the conduction band in In_2O_3.[14] This means that donor defects on or near the surface contribute to a highly conducting accumulation layer. A combined theoretical and experimental study suggested that such surface defects might dominate the conduction properties of thin-film In_2O_3.[15] Specifically, an oxygen vacancy on the surface was calculated to have a donor level nearly degenerate with the surface conduction band minimum. Surface conduction layers have also been measured in ZnO.[16,17]

[a]Address all correspondence to this author.
e-mail: mattmcc@wsu.edu
DOI: 10.1557/jmr.2012.137

 © Materials Research Society 2012

https://doi.org/10.1557/jmr.2012.137 Published online by Cambridge University Press

Surface states are especially important in nanocrystals, due to their high surface-to-volume ratio. The sensitivity of these states to the surrounding environment provides the basis for gas-sensing applications.[18] In general, surface states are complicated, and probably involve impurities such as hydrogen. In ZnO nanocrystals, a red luminescence band has been attributed to intra-gap surface states.[19,20] The electrical conductivity of such nanocrystals is extremely sensitive to hydrogen exposure, which increases free-electron concentrations by several orders of magnitude.[21]

In addition to electronic applications, oxides are also used in hydrogen fuel cells. In a solid-oxide fuel cell (SOFC), oxygen ions (O^{2-}) are produced at the air electrode. The O^{2-} ions migrate through the solid oxide electrolyte until they reach the fuel electrode, where they combine with hydrogen to produce water. Oxide materials with high concentrations of oxygen vacancies are desirable, for high oxygen conductivity.[22] Yttria-stabilized zirconia (YSZ) is a preferred material for SOFCs. Another type of electrolyte is a proton conductor, which is typically a perovskite oxide such as barium cerium oxide ($BaCeO_3$).[23] Oxides may also provide a means of hydrogen production, via photochemical splitting of water. In this process, a solar photon produces an electron and hole, which catalyze the formation of H_2 and O_2. Titania (TiO_2) was the first oxide used for this purpose.[24] Other materials include titanates, tantalates, and niobates.[25]

Hydrogen is usually present in oxide materials and can have a strong effect on the electrical conductivity. Two types of hydrogen donors are interstitial hydrogen, in which the proton forms an O–H bond with a host oxygen atom, and substitutional hydrogen, where the proton occupies an oxygen vacancy. Hydrogen may also exist as H_2 molecules, which are electrically neutral and, unlike O–H pairs, do not absorb infrared (IR) light. Finally, hydrogen can form complexes with acceptor dopants and cation vacancies. By attaching to dangling bonds, hydrogen fully or partially passivates the acceptor levels. The resulting reduction in ionized impurity scattering improves electrical mobility in *n*-type samples.

Depending on the position of the Fermi level, the equilibrium charge state of interstitial hydrogen is +1 or −1. The position of the H(+/−) level defines the point at which hydrogen goes from being a donor to an acceptor. If the Fermi level is above the H(+/−) level, then hydrogen acts as an acceptor and assumes a −1 charge state. If the Fermi level lies below the H(+/−) level, hydrogen is a donor and has a charge of +1 (i.e., it is a proton). Theoretical studies have suggested that the H(+/−) level is "universal" and does not depend on the details of the host lattice.[26,27] Qualitatively, the low conduction band (high electron affinity) of oxide semiconductors means that hydrogen tends to act as a donor. Muons, which act as analogs of hydrogen, have been used to probe this property in many semiconductors.[28] Muonium was shown to be a shallow donor in In_2O_3 and SnO_2,[29] cadmium oxide (CdO),[30] and Ga_2O_3.[31]

Figure 1 shows the H(+/−) level according to two theoretical studies and muon-implantation experiments. The valence-band offsets were taken from the theory[26,27] whereas the energy values are relative to vacuum, according to Ref. 28. One can see that there is a spread of almost 1 eV in the reported H(+/−) values. Furthermore, a recent theoretical study suggests that H(+/−) levels in various oxides are not well aligned, but are scattered over ~2 eV.[32] Resolving these apparent discrepancies will be an important topic for future research.

Section II discusses the presence of hydrogen in several oxide materials, with an emphasis on the microscopic structure of hydrogen complexes in bulk crystals. Fourier transform infrared (FTIR) spectroscopy is the preferred method for studying hydrogen vibrational modes. In this article, vibrational frequencies are the values at low temperatures (5–12 K) unless noted otherwise.

II. SPECIFIC MATERIALS

A. ZnO

ZnO has the wurtzite crystal structure and is relatively easy to grow in bulk or thin-film form.[33,34] As noted in Sec. I, ZnO is an alternative to ITO for transparent contacts in solar cells[35] and transparent electronics.[36] It is also an efficient light emitter, with a band gap of ~3.4 eV at room temperature, making it a candidate for solid-state lighting. The past decade of research has uncovered many interesting defect properties, most of which are also relevant to other oxides.

The status of available information on defects in ZnO was reviewed in 2009 by McCluskey and Jokela.[37] As discussed in their article under reference, numerous calculations have revealed that oxygen vacancies are deep

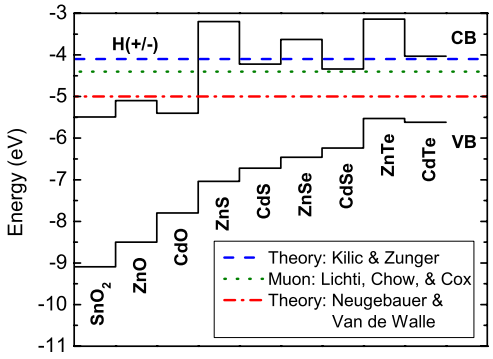


FIG. 1. Alignment of the H(+/−) level for interstitial hydrogen in various semiconductors. LDA calculations were performed by Kiliç and Zunger[27] and Van de Walle and Neugebauer.[26] Muon implantation experiments are from Lichti, Chow, and Cox.[28]

https://doi.org/10.1557/jmr.2012.137 Published online by Cambridge University Press

double donors (e.g., Refs. 38–41). The oxygen vacancy is an example of a "negative *U*" defect, in which the neutral or +2 charge state is always energetically preferred over the +1 charge state. When the Fermi level is above the (0/2+) donor level, the oxygen vacancy is occupied and neutral. When the Fermi level is below the (0/2+) level, the donor is empty and has a charge of +2. The (0/2+) level is estimated to lie 1–2 eV below the conduction band minimum. At thermal equilibrium, such a deep level contributes essentially zero free electrons at room temperature. Electron paramagnetic resonance (EPR) experiments,[42] combined with illumination by visible light,[43] have supported the theoretical claim that oxygen vacancies are deep donors.

Another native defect, the zinc interstitial, has also been proposed as a source of *n*-type conductivity in ZnO. Whereas it is probably indeed a shallow donor, calculations have shown that the zinc interstitial has a low migration barrier.[44] At room temperature, it will simply migrate to the surface or become trapped by a defect. This is in agreement with EPR experiments that show zinc interstitials to be unstable at room temperature.[42]

With native defects out of the picture, hydrogen is considered to be an important contributor to *n*-type conductivity. There are two forms in which hydrogen acts as a shallow donor, interstitial and substitutional hydrogen. Interstitial hydrogen forms an O–H bond that gives rise to a bond-stretching peak in the IR absorption spectrum. There are two different interstitial hydrogen donors, with peaks at 3326 cm^{-1} (McCluskey et al.[45]) and 3611 cm^{-1} (Lavrov et al.[46]). Whereas it has been proposed that the 3326 cm^{-1} line may be an O–H pair adjacent to a calcium impurity,[47–49] this model has not been established experimentally. Both interstitial hydrogen donors are unstable at room temperature, decaying away after a few weeks (Fig. 2).[50] Some of the hydrogen atoms form H_2 molecules, which are electrically neutral and "hidden" from IR spectroscopy.[51,52] Since interstitial donors are unstable, they are not responsible for the prevailing *n*-type conductivity in ZnO samples.

Substitutional hydrogen, in contrast, is believed to be a shallow donor that is stable to ~500 °C.[51] First-principles calculations showed that the hydrogen atom sits in an oxygen vacancy and forms weak bonds with the neighboring zinc atoms.[53] Because the bonds are weak, its predicted vibrational frequency is low (~800 cm^{-1}), lying in a spectral region with strong IR two-phonon and free-carrier absorption. For this reason, detecting substitutional hydrogen by IR spectroscopy presents a technical challenge. To our knowledge, substitutional hydrogen has not been observed with IR spectroscopy in other oxides either, presumably for the same reason. Photoluminescence spectra at low temperatures show several sharp lines corresponding to substitutional donors in ZnO.[54] The "I_4" line has been assigned to substitutional hydrogen donors.[53,55]

Along with its role as a shallow donor, hydrogen also passivates acceptors. In ZnO, the zinc vacancy is a double acceptor and is fully passivated by two hydrogen atoms. In essence, the hydrogen atoms provide the electrons that were taken away by the missing zinc atom. The protons then bind to oxygen atoms, resulting in two IR absorption peaks.[46] Hydrogen also has been known to passivate the deep acceptors copper[56] and lithium.[57,58] In both complexes, hydrogen attaches to an oxygen atom, forming an O–H bond.

Nitrogen acceptors are passivated by hydrogen in bulk ZnO grown in ammonia by chemical vapor transport[59] and in thin films grown by metalorganic chemical vapor deposition.[60] Through isotopic substitution, Jokela and McCluskey showed that the IR absorption peak at 3151 cm^{-1} corresponds to the bond-stretching mode of a N–H pair (Fig. 3).[61] The local vibrational mode frequency agreed with a theoretical model, in which the hydro-

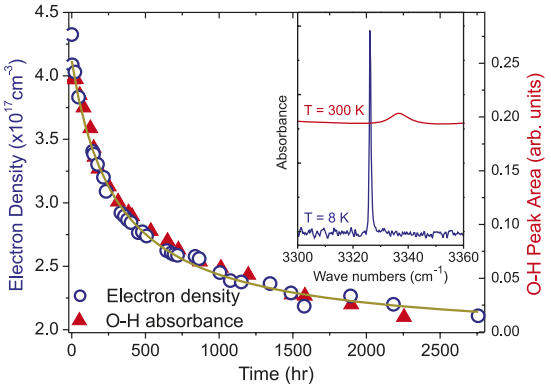


FIG. 2. Free-electron density and O–H peak area for interstitial hydrogen donors in ZnO, at room temperature. The decay over time shows that interstitial donors are unstable.[50] Inset: O–H absorption peak at 8 K and 300 K.

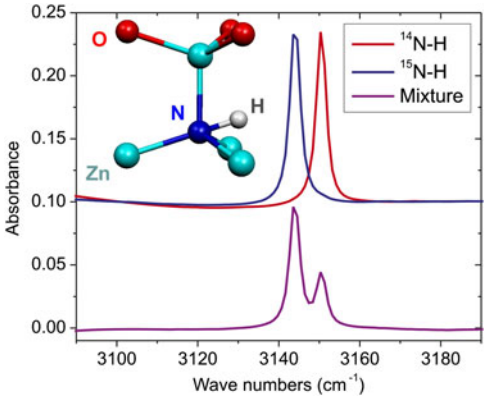


FIG. 3. IR spectra (8 K) of N–H pairs in ZnO, for samples grown in $^{14}NH_3$, $^{15}NH_3$, or a mixture of $^{14}ND_3$ and $^{15}NH_3$.[61] The higher mass of the ^{15}N isotope results in a slightly lower vibrational frequency. N-D peaks are not shown. Inset: ball-and-stick model.[62]

https://doi.org/10.1557/jmr.2012.137 Published online by Cambridge University Press

gen attaches to the nitrogen acceptor in an "antibonding" orientation.[62]

The study of N–H complexes was essential for understanding the nature of nitrogen acceptors in ZnO. As reviewed in Ref. 37, numerous theoretical and experimental reports claimed that nitrogen is a shallow acceptor dopant that could produce *p*-type material. However, more recent calculations have indicated that nitrogen is a *deep* acceptor with a (0/-) level over 1 eV above the valence-band maximum.[63,64] To test the theory, experiments were performed on bulk, single-crystal ZnO:N samples that were grown in an ammonia ambience.[65] In these samples, the majority of the nitrogen acceptors were passivated. To activate the nitrogen acceptors, the samples were annealed, causing the N–H pairs to break up. This led to a decrease in the N–H peak intensity and an increase in "red" luminescence centered at ~730 nm (1.70 eV). The red luminescence is in agreement with the predictions of the deep-acceptor model.[63] These results provided evidence that nitrogen is a deep acceptor in ZnO and cannot lead to *p*-type conductivity.

Regarding hydrogen diffusion, experiment and theory are at odds. Experimentally, a hydrogen migration barrier of ~1 eV has been found by Mollwo,[66] Thomas and Lander,[67] and Nickel.[68] This value concurs with the temperature-dependent decay of interstitial hydrogen donors, which has activation energy of 0.96 eV.[50] However, local density approximation (LDA) calculations predict a much lower migration barrier of 0.4–0.5 eV.[69,70] The reason for this major discrepancy is not currently known.

B. SnO_2

Tin oxide, also known as stannic oxide or cassiterite in its mineral form, has the rutile crystal structure and a direct band gap of 3.6 eV.[71] Fluorine-doped SnO_2 is used as a transparent electrode for thin-film amorphous silicon– and cadmium telluride (CdTe)-based solar cells[72] and dye-sensitized solar cells.[73] Transparent thin-film transistors have also been fabricated.[74] As discussed in Sec. I, SnO_2 coatings are used to improve the energy efficiency of windows, by transmitting visible light while reflecting IR light.[75] They are also used as transparent electrodes in electrochromic windows, in which the window transparency is controlled by an applied voltage.[76] Finally, SnO_2 is used in gas-sensing applications, in which the conductivity changes in the presence of specific gas molecules.[77] The sensitivity to molecules such as carbon monoxide increases significantly when SnO_2 particles have a diameter smaller than 10 nm.[78]

As with many other oxides, the prevailing assumption that oxygen vacancies are responsible for *n*-type conductivity was challenged by DFT calculations.[79] These calculations estimated that the (0/2+) donor level is ~1.8 eV above the valence band maximum, which is in the middle of the band gap. Such a deep level cannot contribute an appreciable concentration of free electrons to the conduction band. The tin interstitial was calculated to have high formation energy in *n*-type material, resulting in a negligible concentration. The authors proposed instead that substitutional and interstitial hydrogen could act as shallow donors in SnO_2.

The theoretical predictions were tested experimentally by annealing bulk, single-crystal SnO_2 in H_2 gas at 600 °C.[80] An IR peak observed at 3156.1 cm^{-1} was attributed to interstitial hydrogen, with the O–H bond aligned perpendicular to the *c*-axis. The hydrogenated samples showed free-carrier absorption and an increase in electrical conductivity, consistent with the shallow-donor nature of interstitial hydrogen. As in ZnO, the O–H peak is unstable, decaying away after a few weeks at room temperature (Fig. 4).

Along with interstitial hydrogen donors, hydrogenated SnO_2 also showed a series of O–H peaks in the 3250–3350 cm^{-1} range. From first-principles calculations, it was proposed that two of these peaks arise from tin vacancies decorated with one hydrogen atom.[80] Two different orientations of the O–H bond result in two different vibrational frequencies (3261.7 and 3282.0 cm^{-1}). The hydrogen atom partially passivates the tin vacancy, converting it into a triple acceptor. The calculated formation energies for these $(V_{Sn}\text{-}H)^{-3}$ defects is low for *n*-type material.

Experiments by Bekisli et al.[81] confirmed the assignment of the 3156.1 cm^{-1} peak to hydrogen donors. By correlating the strength of this peak with that of free-carrier absorption, the authors determined that a second donor, probably substitutional hydrogen, was stable to 600 °C. The properties of interstitial and substitutional hydrogen donors are remarkably similar to those in ZnO. Through systematic IR polarization spectroscopy, they assigned the peaks in the 3250–3350 cm^{-1} range to defects containing

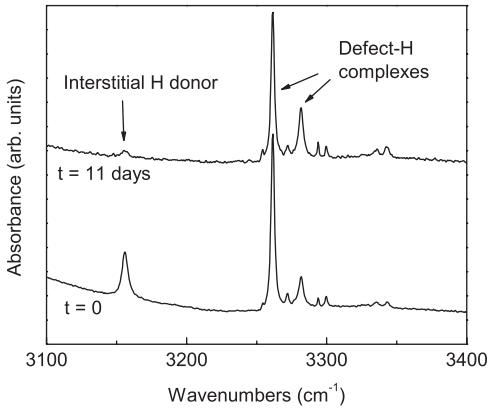


FIG. 4. IR spectra (10 K) of O–H peaks from interstitial hydrogen donors and defect-hydrogen complexes in SnO_2.[80] The top spectrum was taken after an 11 day "anneal" at room temperature.

https://doi.org/10.1557/jmr.2012.137 Published online by Cambridge University Press

one or two hydrogen atoms. All but two lines were polarized perpendicular to the *c*-axis.

First-principles calculations by Varley et al.[82] showed that the acceptors aluminum, gallium, and indium readily substitute for tin, perhaps providing a way toward *p*-type doping in SnO_2. They are all passivated by hydrogen, resulting in O–H bonds that should give rise to well-defined vibrational peaks in the IR spectrum. To our knowledge, however, these acceptor-hydrogen complexes have not been observed experimentally.

C. TiO_2

Titanium dioxide or titania has an indirect band gap of 3.0 eV in the rutile structure and 3.2 eV in the anatase structure.[83] It is widely used as a white pigment in paint. TiO_2 surfaces, especially the well-characterized rutile (110) surface, are used in photocatalytic processes such as water splitting (Sec. I) and photodegradation of organic molecules.[84] The surface adsorption of various organic species has been studied extensively with FTIR spectroscopy.[85] TiO_2 is a preferred material for photoelectrochemical solar cells.[86] In these devices, sunlight creates an electron and hole in the TiO_2. The electron travels through an external circuit whereas the hole is "scavenged" by a molecule in the electrolyte. Dye-sensitized solar cells use a monolayer of dye molecules to push the absorption profile into the visible.[87]

Rutile TiO_2 shows various hydrogen vibrational modes, including one with a frequency 3290 cm^{-1} that corresponds to an O–H bond aligned perpendicular to the *c*-axis.[88] Herklotz et al.[89] investigated the fine structure of this mode and its temperature dependence. They attributed two IR absorption peaks, at 3288.3 and 3292.0 cm^{-1}, to the neutral charge state, and a mode at 3287.4 cm^{-1} to the +1 charge state. As the sample was warmed up, the increase in the 3287.4 cm^{-1} line was correlated with an increase in free-carrier absorption. These results suggest a shallow donor with ionization energy of 10 meV. The experimental work is in contrast to the calculations of Filippone et al., which predicted that interstitial hydrogen should be a deep donor.[90] Other calculations, however, found that interstitial hydrogen is a shallow donor in TiO_2.[27,91,92]

The vibrational lifetime of the O–H bond-stretching mode provides information that is relevant to hydrogen diffusion. IR pump-probe experiments measured the temperature dependence of the ground-state recovery lifetime.[93] The shape of the lifetime-versus-temperature curves suggest that the O–H stretch mode quickly couples to a wag mode, which enables it to migrate to a neighboring oxygen site. This model implies that IR light can lead to a giant enhancement of hydrogen migration in TiO_2.

The theoretical situation for oxygen vacancies is an area of some disagreement. DFT calculations using the generalized gradient approximation (GGA) show that the +2 charge state of the oxygen vacancy is energetically preferred for all values of the Fermi level within the band gap; i.e., it acts as a shallow double donor.[92,94] However, DFT calculations, using a local spin density + *U* method, find that the oxygen vacancy is a deep donor. We note that this latter technique was the same one that also found hydrogen to be a deep donor.[90]

D. In_2O_3 and Ga_2O_3

As discussed in Sec. I, In_2O_3 is the preferred TCO for flat-panel displays and other applications. Despite its popularity and success, relatively little is known about the properties of hydrogen impurities. In_2O_3 has the bixbyite crystal structure, with 80 atoms in the conventional cell. Although it has a direct band gap of 2.7 eV,[95] strong dipole-allowed absorption occurs ~1 eV above this value, making it quite transparent up to ~3.7 eV. Koida et al.[96] demonstrated that hydrogen doping of sputtered films resulted in free-electron concentrations of 3×10^{20} cm^{-3} and mobilities as high as 130 $cm^2/V{\cdot}s$. Calculations by Limpijumnong et al.[97] indicated that substitutional and interstitial hydrogen act as shallow donors, in agreement with experiment. Researchers have exploited the effect of hydrogen on conductivity, using nanocrystalline In_2O_3 thin films as hydrogen gas sensors.[98] The (0/2+) donor level of the oxygen vacancy was calculated to lie close to the experimental conduction-band minimum, suggesting that it may act as a shallow donor.[99]

β-Ga_2O_3 has a monoclinic crystal structure and a direct band gap of 4.9 eV, giving it transparency well into the UV.[100] DFT calculations indicate that oxygen vacancies are deep donors, whereas interstitial and substitutional hydrogen are shallow donors.[101] Whereas isolated cation vacancies are energetically unfavorable in SnO_2 and In_2O_3, gallium vacancies have low formation energy in Ga_2O_3.[13] In the presence of hydrogen, however, the formation energies are reduced and vacancy-hydrogen complexes may form in all three materials.

E. $SrTiO_3$

$SrTiO_3$ is a perovskite oxide (Fig. 5) with an indirect band gap of 3.25 eV[102] and is commonly used as a substrate for oxide thin films, including high-T_c superconductors.[103] The observation of blue light emission in irradiated $SrTiO_3$ suggests potential optoelectronic applications.[104] The cubic perovskite structure undergoes a symmetry-lowering transition to a tetragonal phase below 105 K, which involves a rotation of the oxygen octahedron with respect to the strontium cage.[105] Its dielectric constant depends strongly on temperature, increasing from a few hundred at room temperature to tens of thousands at low temperatures. The dielectric screening of ionized impurities at low temperature contributes to excellent

https://doi.org/10.1557/jmr.2012.137 Published online by Cambridge University Press

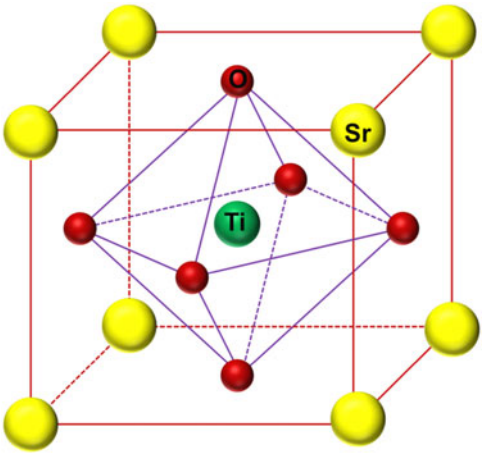


FIG. 5. Perovskite structure of $SrTiO_3$.

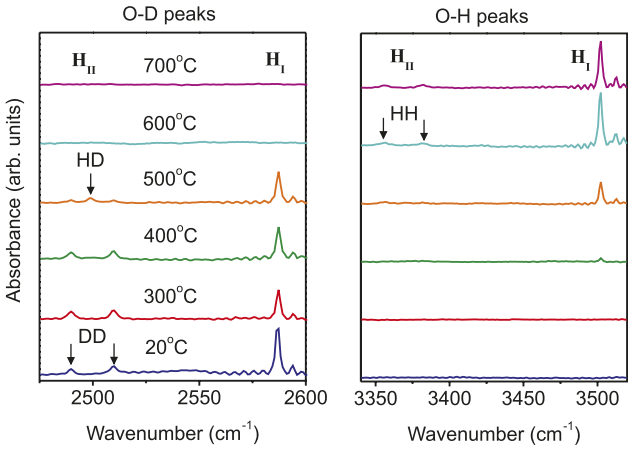


FIG. 6. IR absorption spectra (200 K) of O-D and O-H peaks in deuterated $SrTiO_3$.[109] Two different complexes are labeled H_I and H_{II}. Above 500 °C, the D atoms are replaced by H, which come from a "hidden hydrogen reservoir" in the sample.

free-electron mobilities.[106] Although *p*-type $SrTiO_3$ has been reported via doping with scandium[107] and indium,[108] the evidence–as with claims of *p*-type ZnO–is far from conclusive.

In as-grown $SrTiO_3$, hydrogen forms an O–H bond with a host oxygen atom, resulting in an IR absorption peak near 3500 cm^{-1} due to the bond-stretching vibration.[105] In samples annealed in hydrogen gas, Tarun and McCluskey[109] investigated this peak, labeled H_I, along with a pair of peaks at 3355 and 3384 cm^{-1}, labeled H_{II}. All the peaks showed an expected isotope shift to lower frequency when samples were annealed in deuterium. When samples were annealed in a mixture of hydrogen and deuterium, new H_{II} peaks appeared. These peaks corresponded to HD centers, showing unambiguously that the H_{II} center contains two hydrogen atoms.

The structures of the hydrogen complexes are not known definitively. Theoretical studies have suggested that the H_I line arises from an isolated hydrogen interstitial[110] whereas H_{II} represents a pair of hydrogen interstitials that are attracted to each other via lattice strain.[111] Tarun and McCluskey[109] attributed H_{II} to a strontium vacancy that is fully passivated by two hydrogen atoms. However, the experimental results cannot exclude the possibility that H_{II} is a titanium vacancy decorated by two hydrogen atoms,[112,113] or two neighboring hydrogen interstitials.[111] Furthermore, one must consider the possibility that the H_I configuration is a defect-hydrogen complex rather than simply isolated hydrogen.[112]

By monitoring the evolution of peaks in deuterated $SrTiO_3$, Tarun and McCluskey[109] provided evidence for "hidden hydrogen," possibly H_2 molecules, in the sample. As shown in Fig. 6, the deuterated sample contains O–D peaks corresponding to the H_I and H_{II} configurations. When the sample is annealed at 500 °C, one can see the appearance of an HD peak. This occurs because a hydrogen atom has come out of its reservoir and replaced a deuterium atom. At the same time, the H_I O–H peak increases, for the same reason. At 600 °C, the released hydrogen atoms have totally replaced the deuterium atoms. Future studies, perhaps involving Raman spectroscopy, will be performed to determine the identity of the hidden hydrogen.

III. CONCLUSIONS

Hydrogen is an impurity that is present in essentially all oxide materials and can have a major effect on electrical properties. Several "universal" phenomena are observed in many, if not all, oxide semiconductors. Interstitial and substitutional hydrogen act as shallow donors, with the substitutional form being much more stable. Oxides often contain "hidden hydrogen," possibly H_2 molecules, that can become mobile and electrically active upon annealing. Hydrogen readily passivates dangling bonds in cation vacancies. In ZnO and $SrTiO_3$, for example, vacancy defects with two hydrogen atoms have been observed. Finally, hydrogen passivates substitutional acceptors such as nitrogen in ZnO. Whereas theories have proposed the existence of a universal donor level for interstitial hydrogen, there is significant disagreement over where this level lies and whether it is really constant for oxide semiconductors.

In the future, improving our understanding of hydrogen in oxide semiconductors could lead to a host of new applications. The challenge of *p*-type doping, in particular, will need to take hydrogen into account, since hydrogen can be expected to aggressively passivate any acceptors in the material. Deliberate passivation of compensating acceptors, on the other hand, could lead to higher electron mobilities in *n*-type TCOs. The structural, electronic, and vibrational properties of vacancy-hydrogen

https://doi.org/10.1557/jmr.2012.137 Published online by Cambridge University Press

complexes in oxides such as titanates are still not well known. These complexes could have a major influence on carrier mobilities and, at high concentrations, may affect phenomena such as ferroelectric phase transitions.

ACKNOWLEDGMENTS

The authors would like to thank A. Janotti, S. Lumpijumnong, J.B. Varley, C.G. Van de Walle, and S.B. Zhang for helpful insights into the theory of oxide semiconductors. Financial support was provided by National Science Foundation Grant No. DMR-1004804 (MDM, MCT) and Department of Energy Grant No. DE-FG02-07ER46386 (STT).

REFERENCES

1. R. Ramesh and D.G. Schlom: Whither oxide electronics? *MRS Bull.* **33**(11), 1006 (2008).
2. J.G. Bednorz and K.A. Müller: Possible high T_c superconductivity in the Ba-La-Cu-O system. *Z. Phys. B: Condens. Matter* **64**, 189–193 (1986).
3. M. Dawber, K.M. Rabe, and J.F. Scott: Physics of thin-film ferroelectric oxides. *Rev. Mod. Phys.* **77**, 1083–1130 (2005).
4. A.P. Ramirez: Colossal magnetoresistance. *J. Phys. Condens. Matter* **9**, 8171 (1997).
5. A. Ohtomo and H.Y. Hwang: A high-mobility electron gas at the $LaAlO_3/SrTiO_3$ heterointerface. *Nature* **427**, 423–426 (2004).
6. A. Facchetti and T. Marks, editors: *Transparent Electronics: From Synthesis to Applications* (Wiley, New York, 2010).
7. H. Kawazoe, H. Yanagi, K. Ueda, and H. Hosono: Transparent *p*-type conducting oxides: Design and fabrication of p-n heterojunctions. *MRS Bull.* **25**(8), 28 (2000).
8. D.S. Ginley and C. Bright: Transparent conducting oxides. *MRS Bull.* **25**(8), 15–18 (2000).
9. A.N. Tiwari, G. Khrypunov, F. Kurdzesau, D.L. Bätzner, A. Romeo, and H. Zogg: CdTe solar cell in a novel configuration. *Prog. Photovoltaics Res. Appl.* **12**, 33–38 (2004).
10. T. Minami: New *n*-type transparent conducting oxides. *MRS Bull.* **25**(8), 38 (2000).
11. P.D.C. King and T.D. Veal: Conductivity in transparent oxide semiconductors. *J. Phys. Condens. Matter* **23**, 334214:1–17 (2011).
12. H.L. Hartnagel, A.L. Dawar, A.K. Jain, and C. Jagadish: *Semiconducting Transparent Thin Films* (Institute of Physics, London, 1995).
13. J.B. Varley, H. Peelaers, A. Janotti, and C.G. Van de Walle: Hydrogenated cation vacancies in semiconducting oxides. *J. Phys. Condens. Matter* **23**, 334212:1–9 (2011).
14. P.D.C. King, T.D. Veal, D.J. Payne, A. Bourlange, R.G. Egdell, and C.F. McConville: Surface electron accumulation and the charge neutrality level in In_2O_3. *Phys. Rev. Lett.* **101**, 116808:1–4 (2008).
15. S. Lany, A. Zakutayev, T.O. Mason, J.F. Wager, K.R. Poeppelmeier, J.D. Perkins, J.J. Berry, D.S. Ginley, and A. Zunger: Surface origin of high conductivities in undoped In_2O_3 thin films. *Phys. Rev. Lett.* **108**, 016802:1–4 (2012).
16. O. Schmidt, P. Kiesel, C.G. Van de Walle, N.M. Johnson, J. Nause, and G.H. Döhler: Effects of an electrically conducting layer at the zinc oxide surface. *Jpn. J. Appl. Phys.* **44**, 7271–7274 (2005).
17. D.C. Look, H.L. Mosbacker, Y.M. Strzhemechny, and L.J. Brillson: Effects of surface conduction on hall-effect measurements in ZnO. *Superlattices Microstruct.* **38**, 406–412 (2005).
18. G. Eranna: *Metal Oxide Nanostructures as Gas Sensing Devices* (CRS Press, Boca Raton, FL, 2012).
19. I. Shalish, H. Temkin, and V. Narayanamurti: Size-dependent surface luminescence in ZnO nanowires. *Phys. Rev. B* **69**, 245401:1–4 (2004).
20. S.T. Teklemichael and M.D. McCluskey: Acceptor and surface states of ZnO nanocrystals: A unified model. *Nanotechnology* **22**, 475703:1–4 (2011).
21. W.M. Hlaing Oo, M.D. McCluskey, J. Huso, and L. Bergman: Infrared and Raman spectroscopy of ZnO nanoparticles annealed in hydrogen. *J. Appl. Phys.* **102**, 043529:1–5 (2007).
22. S.C. Singhal: Science and technology of solid-oxide fuel cells. *MRS Bull.* **25**(3), 16–21 (2000).
23. T. Norby: Proton conductivity in perovskite oxides, in *Perovskite Oxides for Solid Oxide Fuel Cells*, edited by T. Ishihara (Springer, New York, NY, 2009); pp. 217–241.
24. A. Fujishima and K. Honda: Electrochemical photolysis of water at a semiconductor electrode. *Nature* **238**, 37–38 (1972).
25. F.E. Osterloh: Inorganic materials as catalysts for photochemical splitting of water. *Chem. Mater.* **20**, 35 (2008).
26. C.G. Van de Walle and J. Neugebauer: Universal alignment of hydrogen levels in semiconductors, insulators and solutions. *Nature* **423**, 626–628 (2003).
27. Ç. Kiliç and A. Zunger: *n*-type doping of oxides by hydrogen. *Appl. Phys. Lett.* **81**, 73–75 (2002).
28. R.L. Lichti, K.H. Chow, and S.F.J. Cox: Hydrogen defect-level pinning in semiconductors: The muonium equivalent. *Phys. Rev. Lett.* **101**, 136403:1–4 (2008).
29. P.D.C. King, R.L. Lichti, Y.G. Celebi, J.M. Gil, R.C. Vilão, H.V. Alberto, J. Piroto Duarte, D.J. Payne, R.G. Egdell, I. McKenzie, C.F. McConville, S.F.J. Cox, and T.D. Veal: Shallow donor state of hydrogen in In_2O_3 and SnO_2: Implications for conductivity in transparent conducting oxides. *Phys. Rev. B* **80**, 081201(R):1–4 (2009).
30. S.F.J. Cox, J.S. Lord, S.P. Cottrell, J.M. Gil, H.V. Alberto, A. Keren, D. Prabhakaran, R. Scheuermann, and A. Stoykov: Oxide muonics: I. Modelling the electrical activity of hydrogen insemiconducting oxides. *J. Phys. Condens. Matter* **18**, 1061–1078 (2006).
31. P.D.C. King, I. McKenzie, and T.D. Veal: Observation of shallow-donor muonium in Ga_2O_3: Evidence for hydrogen-induced conductivity. *Appl. Phys. Lett.* **96**, 062110:1–3 (2010).
32. K. Xiong, J. Robertson, and S.J. Clark: Behavior of hydrogen in wide band gap oxides. *J. Appl. Phys.* **102**, 083710:1–13 (2007).
33. Ü. Özgür, Ya.I. Alivov, C. Liu, A. Teke, M.A. Reshchikov, S. Doğan, V. Avrutin, S-J. Cho, and H. Morkoç: A comprehensive review of ZnO materials and devices. *J. Appl. Phys.* **98**, 041301:1–103 (2005).
34. S.J. Pearton, D.P. Norton, K. Ip, Y.W. Heo, and T. Steiner: Recent advances in processing of ZnO. *J. Vac. Sci. Technol., B* **22**, 932–948 (2004).
35. A. Nuruddin and J.R. Abelson: Improved transparent conductive oxide/p(+)/i junction in amorphous silicon solar cells by tailored hydrogen flux during growth. *Thin Solid Films* **394**, 49–63 (2001).
36. J.F. Wager: Transparent electronics. *Science* **300**, 1245–1246 (2003).
37. M.D. McCluskey and S.J. Jokela: Defects in ZnO. *J. Appl. Phys.* **106**, 071101:1–13 (2009).
38. A.F. Kohan, G. Ceder, D. Morgan, and C.G. Van de Walle: First-principles study of native point defects in ZnO. *Phys. Rev. B* **61**, 15019–15027 (2000).
39. P. Erhard, K. Albe, and A. Kelin: First-principles study of intrinsic point defects in ZnO: Role of band structure, volume relaxation, and finite-size effects. *Phys. Rev. B* **73**, 205203:1–9 (2006).
40. S. Lany and A. Zunger: Dopability, intrinsic conductivity, and nonstoichiometry of transparent conducting oxides. *Phys. Rev. Lett.* **98**, 045501:1–4 (2007).

https://doi.org/10.1557/jmr.2012.137 Published online by Cambridge University Press

41. T.R. Paudel and W.R.L. Lambrecht: First-principles calculation of the O vacancy in ZnO: A self-consistent gap-corrected approach. *Phys. Rev. B* **77**, 205202:1–9 (2008).
42. L.S. Vlasenko and G.D. Watkins: Optical detection of electron paramagnetic resonance for intrinsic defects produced in ZnO by 2.5-MeV electron irradiation *in situ* at 4.2 K. *Phys. Rev. B* **72**, 035203:1–12 (2005).
43. S.M. Evans, N.C. Giles, L.E. Halliburton, and L.A. Kappers: Further characterization of oxygen vacancies and zinc vacancies in electron-irradiated ZnO. *J. Appl. Phys.* **103**, 043710:1–7 (2008).
44. A. Janotti and C.G. Van de Walle: Native point defects in ZnO. *Phys. Rev. B* **76**, 165202:1–22 (2007).
45. M.D. McCluskey, S.J. Jokela, K.K. Zhuravlev, P.J. Simpson, and K.G. Lynn: Infrared spectroscopy of hydrogen in ZnO. *Appl. Phys. Lett.* **81**, 3807–3809 (2002).
46. E.V. Lavrov, J. Weber, F. Börrnert, C.G. Van de Walle, and R. Helbig: Hydrogen-related defects in ZnO studied by infrared absorption spectroscopy. *Phys. Rev. B* **66**, 165205:1–7 (2002).
47. M.D. McCluskey and S.J. Jokela: Sources of *n*-type conductivity in ZnO. *Physica B* **401–402**, 355–357 (2007).
48. X.B. Li, S. Limpijumnong, W.Q. Tian, H.B. Sun, and S.B. Zhang: Hydrogen in ZnO revisited: Bond center versus antibonding site. *Phys. Rev. B* **78**, 113203:1–4 (2008).
49. J. Bang, E-A. Choi, and K.J. Chang: The effect of impurities on hydrogen bonding site and local vibrational frequency in ZnO. *J. Appl. Phys.* **106**, 053522:1–5 (2009).
50. S.J. Jokela and M.D. McCluskey: Structure and stability of O–H donors in ZnO from high-pressure and infrared spectroscopy. *Phys. Rev. B* **72**, 113201:1–4 (2005).
51. G.A. Shi, M. Saboktakin, M. Stavola, and S.J. Pearton: "Hidden hydrogen" in as-grown ZnO. *Appl. Phys. Lett.* **85**, 5601–5603 (2004).
52. E.V. Lavrov, F. Herklotz, and J. Weber: Identification of hydrogen molecules in ZnO. *Phys. Rev. Lett.* **102**, 185502:1–4 (2009).
53. A. Janotti and C.G. Van de Walle. Hydrogen multicenter bonds. *Nat. Mater.* **6**, 44–47 (2007).
54. B.K. Meyer, H. Alves, D.M. Hoffman, W. Kriegseis, D. Forster, F. Bertram, J. Christen, A. Hoffman, M. Strassburg, M. Dworzak, U. Haboeck, and A.V. Rodina: Bound exciton and donor-acceptor pair recombinations in ZnO. *Phys. Status Solidi B* **241**, 231–260 (2004).
55. E.V. Lavrov, F. Herklotz, and J. Weber: Identification of two hydrogen donors in ZnO. *Phys. Rev. B* **79**, 165210:1–13 (2009).
56. F.G. Gärtner and E. Mollwo: IR absorption of OH and OD centers and OH/OH, OD/OD, and OH/OD complexes in Cu-doped ZnO single crystals. *Phys. Status Solidi B* **89**, 381–388 (1978).
57. L.E. Halliburton, L.J. Wang, L.H. Bai, N.Y. Garces, N.C. Giles, M.J. Callahan, and B.G. Wang: Infrared absorption from OH^- ions adjacent to lithium acceptors in hydrothermally grown ZnO. *J. Appl. Phys.* **96**, 7168–7172 (2004).
58. G.A. Shi, M. Stavola, and W. Beall Fowler: Identification of an OH–Li center in ZnO: Infrared absorption spectroscopy and density functional theory. *Phys. Rev. B* **73**, 081201:1–3 (2006).
59. S.J. Jokela and M.D. McCluskey: Unambiguous identification of nitrogen–hydrogen complexes in zinc oxide. *Phys. Rev. B* **76**, 193201:1–4 (2007).
60. O.S. Kumar, E. Watanabe, R. Nakai, N. Nishimoto, and Y. Fujita: Growth of nitrogen-doped ZnO films by MOVPE using diisopropyl zinc and tertiary-butanol. *J. Cryst. Growth* **298**, 491–494 (2007).
61. S.J. Jokela and M.D. McCluskey: Structure and stability of N–H complexes in single-crystal ZnO. *J. Appl. Phys.* **107**, 113536:1–5 (2010).
62. X. Li, B. Keyes, S. Asher, S.B. Zhang, S-H. Wei, T.J. Coutts, S. Limpijumnong, and C.G. Van de Walle: Hydrogen passivation effect in nitrogen-doped ZnO thin films. *Appl. Phys. Lett.* **86**, 122107:1–3 (2005).
63. J.L. Lyons, A. Janotti, and C.G. Van de Walle: Why nitrogen cannot lead to *p*-type conductivity in ZnO. *Appl. Phys. Lett.* **95**, 252105:1–3 (2009).
64. S. Lany and A. Zunger: Generalized Koopmans density functional calculations reveal the deep acceptor state of N_O in ZnO. *Phys. Rev. B* **81**, 205209:1–5 (2010).
65. M.C. Tarun, M. Zafar Iqbal, and M.D. McCluskey: Nitrogen is a deep acceptor in ZnO. *AIP Adv.* **1**, 022105:1–7 (2011).
66. E. Mollwo: The effect of hydrogen on the conductivity and luminescence of zincoxide crystals. *Z. Phys.* **138**, 478–488 (1954).
67. D.G. Thomas and J.J. Lander: Hydrogen as a donor in zinc oxide. *J. Chem. Phys.* **25**, 1136–1142 (1956).
68. N.H. Nickel: Hydrogen migration in single crystal and polycrystalline zinc oxide. *Phys. Rev. B* **73**, 195204:1–9 (2006).
69. M.G. Wardle, J.P. Goss, and P.R. Briddon: First-principles study of the diffusion of hydrogen in ZnO. *Phys. Rev. Lett.* **96**, 205504:1–4 (2006).
70. J. Bang and K.J. Chang: Diffusion and thermal stability of hydrogen in ZnO. *Appl. Phys. Lett.* **92**, 132109:1–3 (2008).
71. M. Batzill and U. Diebold: The surface and materials science of tin oxide. *Prog. Surf. Sci.* **79**, 47–154 (2005).
72. A.E. Delahoy and S. Guo: Transparent conducting oxides for photovoltaics. In *Handbook of Photovoltaic Science and Engineering*, 2nd ed.; A. Luque and S. Hegedus ed.; John Wiley & Sons Ltd., UK, 2011; pp. 716–796.
73. N. Anscombe: Solar cells that mimic plants. *Nat. Photonics* **5**, 266–267 (2011).
74. R.E. Presley, C.L. Munsee, C-H. Park, D. Hong, J.F. Wager, and D.A. Keszler: Tin oxide transparent thin-film transistors. *J. Phys. D* **37**, 2810–2813 (2004).
75. B.G. Lewis and D.C. Paine: Applications and processing of transparent conducting oxides. *MRS Bull.* **25**(8), 22–27 (2000).
76. R.G. Gordon: Criteria for choosing transparent conductors. *MRS Bull.* **25**(8), 52–57 (2000).
77. W. Göpel and K.D. Schierbaum: SnO_2 sensors: Current status and future prospects. *Sens. Actuators, B* **26–27**, 1–12 (1995).
78. F. Lu, Y. Liu, M. Dong, and X. Wang: Nanosized tin oxide as the novel material with simultaneous detection towards CO, H_2 and CH_4. *Sens. Actuators, B* **66**, 225–227 (2000).
79. A.K. Singh, A. Janotti, M. Scheffler, and C.G. Van de Walle: Sources of electrical conductivity in SnO_2. *Phys. Rev. Lett.* **101**, 055502:1–4 (2008).
80. W.M. Hlaing Oo, S. Tabatabaei, M.D. McCluskey, J.B. Varley, A. Janotti, and C.G. Van de Walle: Hydrogen donors in SnO_2 studied by infrared spectroscopy and first-principles calculations. *Phys. Rev. B* **82**, 193201:1–4 (2010).
81. F. Bekisli, M. Stavola, W. Beall Fowler, L. Boatner, E. Spahr, and G. Lüpke: Hydrogen impurities and shallow donors in SnO_2 studied by infrared spectroscopy. *Phys. Rev. B* **84**, 035213:1–8 (2011).
82. J.B. Varley, A. Janotti, A.K. Singh, and C.G. Van de Walle: Hydrogen interactions with acceptor impurities in SnO_2: First-principles calculations. *Phys. Rev. B* **79**, 245206:1–4 (2009).
83. L. Kavan, M. Grätzel, S.E. Gilbert, C. Klemenz, and H.J. Scheel: Electrochemical and photoelectrochemical investigation of single-crystal anatase. *J. Am. Chem. Soc.* **118**, 6716–6723 (1996).
84. U. Diebold: The surface science of titanium dioxide. *Surf. Sci. Rep.* **48**, 53–229 (2003).
85. L. Ojamäe, C. Aulin, H. Pedersen and P-O. Käll: IR and quantum-chemical studies of carboxylic acid and glycine adsorption on

https://doi.org/10.1557/jmr.2012.137 Published online by Cambridge University Press

rutile TiO_2 nanoparticles. *J. Colloid Interface Sci.* **296**, 71–78 (2006).
86. M. Grätzel: Photoelectrochemical cells. *Nature* **414**, 338–344 (2001).
87. B. O'Regan and M. Grätzel: A low-cost, high-efficiency solar cell based on dye-sensitized colloidal TiO_2 films. *Nature* **353**, 737–740 (1991).
88. B. Soffer: Studies of the optical and infrared absorption spectra of rutile single crystals. *J. Chem. Phys.* **35**, 940–945 (1961).
89. F. Herklotz, E.V. Lavrov, and J. Weber: Infrared absorption of the hydrogen donor in rutile TiO_2. *Phys. Rev. B* **83**, 235202:1–5 (2011).
90. F. Filippone, G. Mattioli, P. Alippi, and A. Amore Bonapasta: Properties of hydrogen and hydrogen-vacancy complexes in the rutile phase of titanium dioxide. *Phys. Rev. B* **80**, 245203:1–8 (2009).
91. P.W. Peacock and J. Robertson: Behavior of hydrogen in high dielectric constant oxide gate insulators. *Appl. Phys. Lett.* **83**, 2025–2027 (2003).
92. T.S. Bjørheim, S. Stølen, and T. Norby: *Ab initio* studies of hydrogen and acceptor defects in rutile TiO_2. *Phys. Chem. Chem. Phys.* **12**, 6817–6825 (2010).
93. E.J. Spahr, L. Wen, M. Stavola, L.A. Boatner, L.C. Feldman, N.H. Tolk, and G. Lüpke: Giant enhancement of hydrogen transport in rutile TiO_2 at low temperatures. *Phys. Rev. Lett.* **104**, 205901:1–4 (2010).
94. E. Cho, S. Han, H-S. Ahn, K-R. Lee, S.K. Kim, and C.S. Hwang: First-principles study of point defects in rutile TiO_{2-x}. *Phys. Rev. B* **73**, 193202:1–4 (2006).
95. A. Bourlange, D.J. Payne, R.G. Egdell, J.S. Foord, P.P. Edwards, M.O. Jones, A. Schertel, P.J. Dobson, and J.L. Hutchison: Growth of In_2O_3(100) on Y-stabilized ZrO_2(100) by O-plasma assisted molecular beam epitaxy. *Appl. Phys. Lett.* **92**, 092117:1–3 (2008).
96. T. Koida, H. Fujiwara, and M. Kondo: Hydrogen-doped In_2O_3 as high-mobility transparent conductive oxide. *Jpn. J. Appl. Phys.* **46**, L685–L687 (2007).
97. S. Limpijumnong, P. Reunchan, A. Janotti, and C.G. Van de Walle: Hydrogen doping in indium oxide: An ab initio study. *Phys. Rev. B* **80**, 193202:1–4 (2009).
98. S. Shukla, S. Seal, L. Ludwig, and C. Parish: Nanocrystalline indium oxide-doped tin oxide thin film as low temperature hydrogen sensor. *Sens. Actuators, B* **97**, 256–265 (2004).
99. P. Reunchan, X. Zhou, S. Limpijumnong, A. Janotti, and C.G. Van de Walle: Vacancy defects in indium oxide: An ab-initio study. *Curr. Appl Phys.* **11**, S296–S300 (2011).
100. M. Orita, H. Ohta, M. Hirano, and H. Hosono: Deep-ultraviolet transparent conductive β-Ga_2O_3 thin films. *Appl. Phys. Lett.* **77**, 4166–4168 (2000).
101. J.B. Varley, J.R. Weber, A. Janotti, and C.G. Van de Walle: Oxygen vacancies and donor impurities in β-Ga_2O_3. *Appl. Phys. Lett.* **97**, 142106:1–3 (2010).
102. K. van Benthem, C. Elsässer, and R.H. French: Bulk electronic structure of $SrTiO_3$: Experiment and theory. *J. Appl. Phys.* **90**, 6156–6164 (2001).
103. M. Kawai, S. Watanabe, and T. Hanada: Molecular beam epitaxy of $Bi_2Sr_2CuO_x$ and $Bi_2Sr_2Ca_{0.85}Sr_{0.15}Cu_2O_x$ ultra thin films at 300°C. *J. Cryst. Growth* **112**, 745–752 (1991).
104. D. Kan, T. Terashima, R. Kanda, A. Masuno, K. Tanaka, S. Chu, H. Kan, A. Ishizumi, Y. Kanemitsu, Y. Shimakawa, and M. Takano: Blue-light emission at room temperature from Ar^+-irradiated $SrTiO_3$. *Nat. Mater.* **4**, 816–819 (2005).
105. D. Houde, Y. Lépine, C. Pépin, S. Jandl, and J.L. Brebner: High-resolution infrared spectroscopy of hydrogen impurities in strontium titanate. *Phys. Rev. B* **35**, 4948–4953 (1987).
106. J. Son, P. Moetakef, B. Jalan, O. Bierwagen, N.J. Wright, R. Engel-Herbert, and S. Stemmer: Epitaxial $SrTiO_3$ films with electron mobilities exceeding 30,000 $cm^2V^{-1}s^{-1}$. *Nat. Mater.* **9**, 482–484 (2010).
107. T. Higuchi, T. Tsukamoto, N. Sata, M. Ishigame, Y. Tezuka, and S. Shin: Electronic structure of *p*-type $SrTiO_3$ by photoemission spectroscopy. *Phys. Rev. B* **57**, 6978–6983 (1998).
108. T. Fix, R. Bali, N. Stelmashenko, and M.G. Blamire: Influence of the dopant concentration in In-doped $SrTiO_3$ on the structural and transport properties. *Solid State Commun.* **146**, 428–430 (2008).
109. M.C. Tarun and M.D. McCluskey: Hydrogen-related defects in strontium titanate. *J. Appl. Phys.* **109**, 063706:1–4 (2011).
110. L. Villamagua, R. Barreto, L.M. Prócel, and A. Stashans: Hydrogen impurity in $SrTiO_3$: structure, electronic properties and migration. *Phys. Scr.* **75**, 374–378 (2007).
111. N. Bork, N. Bonanos, J. Rossmeisl, and T. Vegge: Thermodynamic and kinetic properties of hydrogen defect pairs in $SrTiO_3$ from density functional theory. *Phys. Chem. Chem. Phys.* **13**, 15256–15263 (2011).
112. J.T. Thienprasert, I. Fongkaew, D.J. Singh, M-H. Du, and S. Limpijumnong: Identification of hydrogen defects in $SrTiO_3$ by first-principles local vibration mode calculations. *Phys. Rev. B.* **85**, 125205:1–5 (2012).
113. J. Varley, A. Janotti, and C.G. Van de Walle. Private communication.

https://doi.org/10.1557/jmr.2012.137 Published online by Cambridge University Press